EUROPEAN RESPIRATORY journal

FLAGSHIP SCIENTIFIC JOURNAL OF ERS

Early View

Original article

Rescue of multiple class II CFTR mutations by elexacaftor+ tezacaftor+ivacaftor mediated in part by the dual activities of Elexacaftor as both corrector and potentiator

Onofrio Laselva, Claire Bartlett, Tarini N.A. Gunawardena, Hong Ouyang, Paul D.W. Eckford, Theo J. Moraes, Christine E. Bear, Tanja Gonska

Please cite this article as: Laselva O, Bartlett C, Gunawardena TNA, *et al*. Rescue of multiple class II CFTR mutations by elexacaftor+ tezacaftor+ivacaftor mediated in part by the dual activities of Elexacaftor as both corrector and potentiator. *Eur Respir J* 2020; in press (https://doi.org/10.1183/13993003.02774-2020).

Rescue of multiple class II CFTR mutations by elexacaftor+ tezacaftor + ivacaftor mediated in part by the dual activities of Elexacaftor as both corrector and potentiator

Onofrio Laselva[1,2], Claire Bartlett[3], Tarini NA Gunawardena[1,3], Hong Ouyang[3], Paul DW Eckford[1], Theo J Moraes[3,4], Christine E Bear[1,2,5] and Tanja Gonska[3,4*]

[1]Programme in Molecular Medicine, Hospital for Sick Children, Toronto, Canada

[2] Department of Physiology, University of Toronto, Toronto, Canada

[3]Programme in Translational Medicine, Hospital for Sick Children, Toronto, Canada

[4] Department of Paediatrics, University of Toronto, Toronto, Canada

[5] Department of Biochemistry, University of Toronto, Toronto, Canada

* Corresponding author address: The Hospital for Sick Children, , 555 University Avenue, room 8415, Toronto, ON, M5G 8X4, Canada.
email: tanja.gonska@sickkids.ca

Keywords: Cystic Fibrosis, personalized medicine, CFTR, elexacaftor, rare mutation, nasal epithelial cells

ABSTRACT

Positive results in preclinical studies of the triple combination of elexacaftor, tezacaftor and ivacaftor, performed in airway epithelial cell cultures obtained from patients harboring F508del-CFTR, translated to impressive clinical outcomes for subjects carrying this mutation in clinical trials and approval of TRIKAFTA^{TM}. Encouraged by this correlation, we were prompted to evaluate the effect of the elexacaftor, tezacaftor and ivacaftor triple combination on primary nasal epithelial cultures obtained from individuals with rare Class II cystic fibrosis causing mutations ; G85E, M1101K and N1303K for which TRIKAFTA^{TM} is not approved. Cultures from individuals homozygous for M1101K responded better than cultures harboring G85E and N1303K after treatment with the triple combination with respect to improvement in regulated channel function and protein processing. A similar genotype specific effect of the triple combination was observed when the different mutations were expressed in HEK-293 cells, supporting the hypothesis that these modulators may act directly on the mutant proteins. Detailed studies in nasal cultures and HEK-293 cells showed that the corrector: elexacaftor, exhibited dual activity as both corrector and potentiator and suggested that the potentiator activity contributes to its pharmacological activity. These preclinical studies using nasal epithelial cultures identified mutation genotypes for which elexacaftor, tezacaftor and ivacaftor may produce clinical responses that are comparable to, or inferior to those observed for F508del-CFTR.

INTRODUCTION

Cystic Fibrosis (CF) is caused by mutations in the cystic fibrosis transmembrane conductance regulator (CFTR) gene, which encodes for an ion channel mediating chloride and bicarbonate transport across epithelial cells. CF Patients suffer of multi-organ disease. However, early mortality is mainly caused by progressive, destructive lung disease [1-3]. Following the clinical success of the first CFTR modulators, ivacafor (VX-770) and lumacaftor (VX-809) [4-6], the Food and Drug Administration (FDA) has recently approved the next generation CFTR modulator (TRIKAFTA™). This highly effective CFTR modulator consists of 2 corrector molecules, elexacaftor (VX-445) and tezacaftor (VX-661), which synergistically help to process misfolded CFTR protein to the cell membrane, and a potentiator, ivacaftor, which increases channel opening [7, 8]. Phase 3 clinical trials with TRIKAFTA™ have shown dramatic improvement in lung function, reduction in pulmonary exacerbations and improvement in the quality of life of patients carrying at least one c.1521_1523delCTT (F508del)-CFTR allele [7, 9].

The F508del-CFTR is the prototypical Class II CFTR mutation resulting in defective CFTR protein trafficking due to protein misfolding, reduced stability of the protein at the cell surface and dysfunctional channel gating [10]. There are rare Class II mutations such as c.3302T>A (M1101K), c.254G>A (G85E), c.1705T>G (Y569D) and c.3909C>G (N1303K), which are found in 0.2%, 0.7%, 0.03% and 2.4% of CFTR2 registered CF patients, respectively (https://cftr2.org). It has been previously published that some of these rare mutations (i.e. M1101K, G85E and N1303K), show a defect in CFTR processing, similar to F508del-CFTR [11, 12]. M1101K and N1303K mutations demonstrated only a modest rescue after lumacaftor correction and ivacaftor potentiation when expressed in heterologous expression systems [13-15].

In the current work, we aimed to evaluate the effect of TRIKAFTA™ on rare Class II CFTR mutations using nasal epithelial cell cultures generated from CF patients homozygous for M1101K, G85E, and N1303K.

MATERIAL AND METHODS

Patients

Nasal epithelial cell cultures were obtained from CF patients enrolled in the Program for Individualized CF Therapy (CFIT) Program (lab.research.sickkids.ca/cfit/;[16]). This study was approved by the Research Ethics Board of the Hospital for Sick Children (REB# 1000044783) and St. Michael's Hospital (REB# 1000044783). All study participants or their guardians signed an informed consent.

Cell culture

Human embryonic kidney (HEK)293 GripTite cells (HEK239) were maintained in DMEM (Wisent, St-Bruno, QC) supplemented with non-essential amino acids (Life Technologies, Waltham, MA) and 10% fetal bovine serum (FBS; Wisent, St-Bruno, QC) at 37 °C and 5% CO_2 as previously described [17]. All CFTR variants used in this study were transiently expressed in HEK293 cells using PolyFect Transfection Reagent (Qiagen, Hilden, Germany), according to the manufacturer's protocol as previously described [18].

16HBE14o- cells, CRISPR/Cas9 edited to express N1303K-CFTR, were obtained from the Cystic Fibrosis Foundation (CFF 16HBEge N1303K-CFTR) [19]. Nasal epithelial cell cultures were generated following nasal brushing of the individual patients as previously described [20, 21].

Nasal epithelial cells were expanded and frozen at passage 1 (P1). These P1 cells were thawed and expanded in Passage 2 using PneumaCult™ Ex-Plus (Stemcell Technologies, Vancouver, Canada) then seeded on collagen coated transwell inserts as passage 3 (6.5 mm diameter, 0.4 μm pore size, Corning, Tewksbury, MA). Once confluent, the cells were cultured for 14 days at an air liquid

interface (ALI) with basal differentiation media (PneumaCult^{TM} ALI, StemCell Tech., Vancouver, Canada) [16, 22, 23] before functional and protein studies were performed.

CFTR channel function in HEK293 and CFF-16HBE14o- N1303K-CFTR cells

HEK293 cells, were seeded in 96-well plates (Costar , Corning, Tewksbury, MA). After 24 hrs the cells were transfected with either M1101K, G85E or N1303K-CFTR constructs and 18 hrs post-transfection were treated with the following CFTR modulators: 0.1% DMSO, 3 μM VX-809, 3 μM VX-809 or 3 μM [S]-VX445+3 μM VX-661 for 24 hrs at 37°C. 16HBE14o- cells were grown at 37°C for 5 days post-confluence on 96-well plate (Costar, Corning, Tewksbury, MA) as previously described [24]. The cells were treated with above listed CFTR modulators 24 hrs before the FLiPR functional assay. Cells were then loaded with blue FLiPR membrane potential dye (Manufacturer details) dissolved in chloride free buffer (136 mM sodium gluconate, 3 mM potassium, gluconate, 10 mM glucose, 20 mM HEPES, pH 7.35, 300 mOsm, at a concentration of 0.5 mg/mL, Molecular Devices), for 30 min at 37°C. The CFTR function was determined using FLIPR Tetra® (Molecular Devices) at 37°C. After establishing a baseline fluorescence read (excitation: 530 nm, emission: 560 nm) for 5 min; CFTR was stimulated using forskolin (10 μM; Sigma) and the potentiators VX-770 (1 μM) or [S]-VX-445 (1 μM). CFTR-mediated depolarization of the plasma membrane was detected as an increase in fluorescence following which the CFTR inhibitor (CFTRinh-172, 10 μM) was added to inactivate CFTR. The peak changes in fluorescence to CFTR agonists were normalized relative to the baseline fluorescence [24, 25].

Ussing chamber studies of primary nasal epithelial cells

Day 14 ALI nasal epithelial cells in 6.5 mm transwells were mounted in circulating Ussing chambers (Physiological Instruments) and measurements to assess CFTR function were performed as previously described [26]. The perfusion bath (126 mM NaCl, 24 mM NaHCO3, 2.13 mM K_2HPO_4, 0.38 mM KH_2PO_4, 1 mM $MgSO_4$ 1 mM $CaCl_2$ and 10 mM glucose) was maintained at a

pH of 7.4, a temperature of 37°C and continuously gassed with a 5% CO_2 / 95% O_2 mixture. Measurements were performed in symmetrical chloride concentrations, in open circuit mode and are presented as transepithelial current (Ieq). The transepithelial resistance was 250+/- 122 Ohmcm^2 for healthy control nasal cells and 330 +/- 130 Ohmcm^2 for CF nasal cells. Before the experiments, cells were treated with 0.1% DMSO, 3 μM VX-809+ 1 μM VX-770, 3 μM VX-661+ 3 μM [R]-VX-445+ 1 μM VX-770 or 3 μM VX-661+ 3 μM [S]-VX-445+1 μM VX-770 for 48 hrs. During the experiment 1 μM VX-770 was also added acutely. CFTR function was determined in presence of amiloride (30 μM, Spectrum Chemical, Gardena, CA) and following cAMP activation with forskolin (IeqFSK, 0.1 or 10 μM for Wt or 10 μM for F508del-, M1101K-, G85E-, N1303K-CFTR, Sigma-Aldrich, Missouri, US). CFTR activity was confirmed as Ieq difference following CFTR inhibition with $CFTR_{Inh-172}$ ($IeqCFTR_{Inh-172}$ 10 μM, EMD Millipore Corp. Massachusetts, US)[20, 27]. The maximal response IeqFSK (μA/cm^2) was calculated as a difference between the steady baseline of the measured Ieq following Amiloride -inhibition and the lowest measured peak Ieq following addition of ivacaftor/elexavactor plus FSK.

Immunoblotting

Day 14 ALI Nasal epithelial cells were lysed in modified radioimmunoprecipitation assay (RIPA) buffer (50 mM Tris-HCl, 150 mM NaCl, 1 mM EDTA, pH 7.4, 0.2% SDS, and 0.1% Triton X-100) containing a protease inhibitor cocktail (Roche, Mannheim, Germany) for 10 min [28]. Soluble fractions were analyzed by SDS-PAGE on 6% Tris-Glycine gels (Life Technologies, California, US). After electrophoresis, the proteins were transferred to nitrocellulose membranes (Bio-Rad, Hercules, CA) and incubated in 5% milk. CFTR bands were detected with human CFTR-specific murine mAb 596 (NBD2, 1024-1211) (UNC, North Carolina, USA) using a 1:500 dilution. The blots were developed with ECL (Amersham) using the Li-Cor Odyssey Fc (LI-COR Biosciences, Lincoln, NE) in a linear range of exposure (2-45 min) [29-31]. Relative levels of CFTR protein

were quantified by densitometry of immunoblots using ImageStudioLite (LI-COR Biosciences, Lincoln, NE).

Compound Description

VX-809, VX-661 and VX-770 were obtained from by Selleck Chemicals; [R]-VX-445 (N-(1,3-dimethylpyrazol-4-yl)sulfonyl-6-[3-(3,3,3-trifluoro-2,2-dimethyl-propoxy)pyrazol-1-yl]-2-[(4R)-2,2,4-trimethylpyrrolidin-1-yl]pyridine-3-carboxamide) and [S]-VX-445 (N-(1,3-dimethylpyrazol-4-yl)sulfonyl-6-[3-(3,3,3-trifluoro-2,2-dimethyl-propoxy)pyrazol-1-yl]-2-[(4S)-2,2,4 trimethylpyrrolidin-1-yl]pyridine-3-carboxamide) MedChemExpress, [24].

Statistical analysis

Data are represented as mean ± standard deviation (SD). Paired two-tailed Student's t-test or one-way ANOVA were used for comparison between groups with a significance level of $p< 0.05$. Data with multiple comparisons were assessed using Tukey's multiple-comparison test with $\alpha=0.05$. GraphPad Prism 7.0 software (San Diego, CA) was used for all statistical tests.

RESULTS

Triple modulator combination VX-445+ VX-661+ VX-770 partially rescues the processing and functional defect of F508del in nasal epithelial cell cultures

Since the triple combination VX-445+ VX-661+ VX-770 was approved by FDA for the CFTR mutant F508del, we first assessed the CFTR response to this drug combination in patient derived nasal epithelial cells from 3 F508del/F508del patients as a benchmark experiment. Due to the absence of detailed information on the enantiomer of VX-445 used in the clinically approved triple drug combination, we tested both the [R]- and [S]-isoforms of VX-445. Treatment with [S]-VX-445+ VX-661+ VX-770 showed a statistically significant increase in Ieq after acute application of

forskolin and VX-770 in F508del/F508del nasal epithelial cells and an even larger increase in $IeqCFTR_{Inh-172}$, a result that is consistent with enhanced constitutive CFTR channel activity following chronic treatment with the potentiator, VX-770. The [R]-enantiomer was less effective in modulating this response (**Figure 1A-C**). Experiments were conducted with chronic and acute application of VX-770 demonstrating that if VX-770 is added chronically, the potentiated forskolin response is smaller than the response if VX-770 is added acutely, together with forskolin (**Figure 1B and C**). This is consistent with reports of the inhibitory effect of chronic VX-770 on the functional expression of F508del-CFTR (**Figure 1A-C**) [32, 33]. As chronic VX-770 treatment is thought to better reflect the clinical pharmacokinetics of these combination drugs, we continued testing the effect of CFTR modulators with chronic application of VX-770. In order to show that the combination of VX-445 and VX-661 and not just VX-661 caused the larger responses when compared to VX-809 treatment, we performed comparative experiments in F508del/F508del nasal epithelial cells between VX-809 and VX-661 and demonstrated no difference between the response (**Figure S1**). Since VX-809 is an integral part of the clinically approved drug ORKAMBI™ we continued use of VX-809 for the rest of the experiments.

Western blot analysis of the treated F508del/F508del nasal epithelial cell cultures showed a significant increase in the mature form (Band C) of the F508del- CFTR protein following treatment with [S]-VX-445+VX-661+VX-770 compared to DMSO treatment and is approximately 70% of Wt-CFTR protein processing (band C/ (band C+ band B)). The [R]-isoform of VX-445 had no effect on CFTR protein expression. These findings support correction of the processing defect of F508del-CFTR in patient derived nasal epithelial cells by [S]-VX-445+VX-661+VX-770 resulting in improved CFTR function (**Figure 1DE**). In order to compare drug responses between different CFTR mutations in a clinically relevant manner, we used the F508del/F508del results as benchmark to study the effect of the triple combination on other Class II mutations. Since the initiation of these experiments, it has been confirmed that the [S]-enantiomer is the clinical compound.

Variable levels of VX-445+ VX-661+ VX-770 rescue are observed for other Class II mutations

We next studied the effect of VX-445+ VX-661+ VX-770 on CFTR function in nasal epithelial cell cultures from patients homozygous for M1101K, G85E or N1303K, respectively. Treatment of nasal epithelial cultures from 3 individuals who are homozygous for M1101K with [S]-VX-445+ VX-661+ VX-770 led to a significant increase in CFTR function, measured as the acute current response to forskolin plus potentiator or as the increase in $IeqCFTR_{Inh-172}$ (**Figure 2A+G-H**). The CFTR response to triple combination exceeded the response observed in nasal epithelial cells from 3 F508del/F508del patients. This functional rescue is supported by an increase in mature CFTR protein. Western blot analysis showed a significant increase in M1101K-CFTR protein processing (band C/ (band C+ band B) following treatment with [S]-VX-445+VX-661+VX-770 relative to DMSO (**Figure 2B+J**). Triple combination with the [R]-enantiomer also increased M1101K-CFTR function, but to a lesser extent (**Figure 2G+H+J**).

Treatment of nasal epithelial cells from 3 subjects who are homozygous for G85E with [S]-VX-445 + VX-661+ VX-770 showed a small, but significant, increase in CFTR function, when measured as the $IeqCFTR_{Inh-172}$–sensitive current and when compared to DMSO treated nasal cells. The [S]-VX-445+ VX+661+ VX-770–mediated increase in $IeqCFTR_{Inh-172}$ reached about half of the $IeqCFTR_{Inh-172}$ increase measured in F508del/F508del nasal epithelial cells (**Figure 2C+G+H+I**). This increase in CFTR function was paralleled by a small but significant increase in G85E-CFTR protein maturation relative to DMSO pretreatment (**Figure 2 D+J**). In this mutation, triple combination with the [R]-enantiomer had no significant effect (**Figure 2G+H+J**).

Nasal cells from 2 patients homozygous for N1303K showed a significant increase in CFTR function measured as the IeqFSK and $IeqCFTR_{Inh-172}$ following 48 hrs treatment with [S]-VX-445+ VX+661+ VX-770 and also acute addition of VX-770 (**Figure 2 E+G+H**). However,

interestingly, there was negligible improvement in N1303K-CFTR protein processing caused by [S]-VX-445+ VX-661+ VX-770 on N1303K-CFTR protein (**Figure 2 F+J**). This suggests that the increase in N1303K-CFTR function did not occur via improved protein processing, rather by potentiation of the function of membrane-residual N1303K proteins. Also, it was interesting to note, that the triple combination treatment with both the [S]- and the [R]-enantiomer had a similar effect.

VX-445 functions as a corrector and a potentiator drug

One way to explain the discrepancy between VX-445+ VX-661+ VX-770 induced increase in N1303K -CFTR function and protein expression is that the combination drugs, perhaps VX-445, exhibits potentiator activity. To test the hypothesis that, in addition to its corrector activity, VX-445 functions as a CFTR potentiator, we first examined the effect of acute addition of [S]-VX-445 on channel function of Wt-CFTR using nasal and bronchial epithelial cells derived from non-CF controls and non-CF lung explants, respectively. Interestingly, the acute addition of [S]-VX-445 increased IeqFSK in both Wt-CFTR nasal and bronchial epithelial cell cultures (**Figure 3A-C**). While, $IeqCFTR_{Inh-172}$ following acute [S]-VX-445 and FSK addition did not show statistically difference compared to acute FSK addition alone in primary nasal epithelial cells (**Figure 3D**), mainly due to the variable levels of constitutive CFTR conductance, acute [S]-VX-445 application significantly increased $IeqCFTR_{Inh-172}$ in primary bronchial epithelial cells (**Figure 3E**). Similarly, acute addition of [S]-VX-445 increased the FSK response of F508del-CFTR after VX-661 rescue in nasal epithelial cultures (**Figure 3F-H**). Pilot studies suggest that the potentiator activity of VX-445 is modified by the phosphorylation status of CFTR. We did not observe potentiation of F508del-CFTR after VX-661 rescue by [S]-VX-445 if it was added after activation with 10 μM forskolin (data not shown). However, as shown in **Figure S2**, we did observe a modest but significant potentiation after addition of 0.1 μM forskolin in Wt-CFTR nasal cultures. Interestingly, a similar

observation was reported by McCarty group showing that VX-770 potentiation activity of CFTR variants is influenced by phosphorylation level [34].

We studied the dose dependence of VX-445 potentiation for F508del-CFTR and the rare Class II mutants in HEK-293 cells after their correction at low temperature (27°C) incubation (**Figure 4A+B**). Of the rare mutants studied, only G85E failed be corrected at low temperature [12]. In this system, VX-445-mediated potentiation of forskolin (10 μM) -activated channel function of F508del-CFTR was measured using the FLiPR, membrane potential dye assay as it facilitated the study of multiple doses simultaneously. For F508del-CFTR, the efficacy of VX-445 as a potentiator was significantly less than VX-770 but this was not the case for all of the mutants studied. In **Figure 4C and D**, we show dose-responses for VX-770 and VX-445 in potentiating M1101K and N1303K. Interestingly, there were differences in the potentiator responses across the F508del, M1101K and N1303K genotypes. The efficacy of VX-445 as a potentiator was less than that of VX-770 for N1303K-CFTR but not for M1101K where the efficacies for the two compounds were similar. Future studies are required to understand the structural basis for the differential potentiator responses amongst genotypes.

Next, we studied the potentiation activity of VX-445 on F508del, M1101K, G85E and N1303K mutants expressed in HEK-293 cells after pre-treatment with VX-661+[S]-VX-445 at 37°C (**Figure 5**). As shown in **Figure 5A**, after correction of F508del-CFTR with VX-661 and [S]-VX-445, the subsequent addition of VX-770 or [S]-VX-445 potentiated its forskolin-dependent channel activity. Regarding the rare mutations, we confirmed the previous findings in nasal epithelial cell cultures, where VX-809 and VX-661 alone did not rescue VX-770 potentiated channel function, but the combination of VX-445 and VX-661 did rescue VX-770 potentiated activity for M1101K, G85E and N1303K. A similar rescue effect was observed using 16HBE14o- cells edited using CRISPR-Cas9 to express the N1303K-CFTR mutant (CFF 16HBEge N1303K-CFTR) (**Figure S3A-B**).

Interestingly, [S]-VX-445 also significantly potentiated the forskolin activated function of VX-661+VX-445-corrected rare variants.

Western blot analysis of HEK293 cells expressing CTFR mutants recapitulated our findings on patient derived nasal cells (**Figure 5D**). Treatment with the corrector VX-809 or VX-661 caused a modest improvement in processing for F508del-CFTR, but not for M1101K or G85E-CFTR expressing cells (**Figure 5D and E**). Interestingly and similarly to what we saw in nasal cells, treatment with [S]-VX-445+ VX-661, did not lead to an increase in mature CFTR protein for N1303K. Consistent with our findings in HEK-293 cells overexpressing N1303K-CFTR, N1303K-CFTR expressing 16HBEge cells also showed functional rescue following treatment with [S]-VX-445+ VX-661+ VX-770 without showing an increase in CFTR protein maturation (**Figure S3C-D**). We suggest that there is sufficient amount of mature glycosylated N1303K-CFTR protein to mediate potentiator induced CFTR channel activity. However, the protein signal of the N1303K-CFTR C band is diffuse in CFF 16HBEge N1303K-CFTR and primary nasal epithelial cells as reported earlier [35].

Lastly, we tested the effect of [S]-VX-445+ VX-661+ VX-770 in nasal cells from 1 patient homozygous for Y596D/Y596D (**Figure S4**) and from 2 patients heterozygous for G542X/N1303K (**Figure S4**). As shown in **Figure S4 and S5**, the drug combination [S]-VX-445+ VX-661+ VX-770 did not elicit any increase of CFTR function in either of these mutations.

To summarize, we observed various effects of the [S]-VX-445+ VX-661+ VX-770 triple combination on the functional rescue of different Class II mutations (**Figure 2I**).

DISCUSSION

In this study we show that the novel triple combination of CFTR modulators, two corrector compounds: VX-445, VX-661 and the potentiator compound: VX-770 contained in TRIKAFTA™ improved processing and channel activity of F508del-CFTR in nasal epithelial cell cultures generated from patients homozygous for the major mutation. This result replicates previous preclinical data obtained using primary bronchial epithelial cell cultures [7] and supports the use of primary nasal epithelial cell cultures to study modulator efficacy. Interestingly, in the current study, we found that the *in-vitro* responses to the triple combination were variable amongst Class II mutation genotypes. These findings prompted in-depth studies of elexacaftor (VX-445) in nasal epithelial cell cultures, wherein we determined that it exhibits two activities, both as a corrector and as a potentiator. Further, these studies support the concept that either or both of elexacaftor's activities could contribute to its rescue effect, depending on the genotype. Given the relative inaccessibility of primary bronchial epithelial cell cultures from individuals who are homozygous for rare processing mutations, our findings support the use of patient-derived nasal epithelial cell cultures for preclinical studies of therapeutic interventions as well as studies on their mechanism of action.

Treatment of CF patients homozygote for F508del with the triple combination TRIKAFTA™ was highly efficacious in clinical trials leading to an improvement in lung function with an increase of 10% in the percent predicted forced expiratory volume in 1 sec (ppFEV1), a decrease in sweat chloride concentration by 45 mmol/L and an improvement in life quality [36]. In preclinical studies using primary bronchial epithelial cell cultures, this combination led to a significant functional rescue of the F508del mutant, which exceeded the rescue achieved with ORKAMBI™ [7]. Hence, the preclinical response size in the bronchial epithelial culture model was predictive of the clinical effect size. Similarly, the *in-vitro* response to this combination in primary nasal epithelial cell cultures from patients homozygous for F508del-CFTR may also provide a biomarker of clinical response. Additional subjects need to be studied, but we propose that the *in-vitro* rescue of

F508del/F508del nasal epithelial cell cultures by the triple combination may set the threshold with which to predict clinical efficacy for individuals bearing rare mutations.

Our comparison of VX-770 potentiated forskolin-dependent currents and the corresponding $CFTR_{Inh-172}$ -sensitive currents in cultures treated chronically with the triple combination (**Figure 2I**), showed that there were variable responses across different genotypes. Interestingly, patient-derived nasal epithelial cell cultures expressing M1101K exhibited a superior functional rescue relative to F508del. Nasal epithelial cell cultures expressing G85E and N1303K exhibited a smaller response. The corresponding studies of mutant protein processing provides insight into possible mechanisms underlying these genotype specific differences. The triple combination caused a significant increase in protein processing relative to pre-treatment with ORKAMBI™ (i.e. VX-809 plus VX-770) for F508del, M1101K and G85E, but not for N1303K. The molecular mechanisms underlying correction by VX-445 was investigated in a recent study by Lukacs [37]. VX-445 stabilized NBD1 in biophysical studies, the authors suggested that it acts directly on this domain in the context of the full-length protein. Its efficacy in correcting rare Class 2 mutations residing in distinct domains supports the idea that it has an allosteric effect to promote multi-domain assembly. The findings of the current paper support these observations and the putative allosteric mechanism of action of VX-445. Future studies are required to determine if differential protein stability at the cell surface accounts for the discrepancy between the magnitude of functional responses to chronic treatment with VX-445+VX-661+ VX-770 seen for M1101K and F508del in nasal epithelial cell cultures versus HEK-293 cells.

Interestingly, for N1303K-CFTR, there was no improvement in protein processing caused by the triple combination relative to VX-809+VX-770 despite a relative improvement in functional rescue. We suggest that this functional rescue by VX-445+ VX-661+ VX-770 reflects potentiation of very low residual surface expression. This potentiation was mediated by both VX-770 and VX-445 (the dual acting corrector, potentiator compound). Interestingly, Phuan and colleagues [38], also showed

functional rescue of N1303K in an HBE cell line expressing N1303K CFTR with the addition of two potentiators alone, with no corrector [38]. They also showed that N1303K-CFTR was effectively potentiated using a combination of specific potentiation modulators in Fischer thyroid rat (FRT) cells as well as in nasal and bronchial epithelial cells from a N1303K/N1303K patient [38, 39]. Recently, we also showed that another combination of molecules provided by Abbvie Pharmaceuticals, a potentiator (referred as AP2) plus a dual-acting corrector-potentiator compounds (referred as AC2.2) evoked functional rescue of N1303K-CFTR without a significant improvement in its processing [35]. Altogether, we are seeing a consistent response of N1303K-CFTR to modulators and these findings support the claim that it is the potentiator activity of VX-445 that is important for functional rescue of this mutant.

In summary, we demonstrated variable responses among Class II genotypes to elexacaftor, tezacaftor and ivacaftor, while identifying the dual activities of VX-445. Our study also highlighted the utility of patient-derived nasal epithelial cell cultures to test drug efficacy and to glean insights regarding the mechanisms underlying drug activity.

ACKNOWLEDGEMENTS

Primary nasal cell cultures were obtained through the CF Canada-Sick Kids Program for Individualized CF Therapy (CFIT). This work was supported by the CFIT Program with funding provided by CF Canada and the Sick Kids Foundation. This work was funded by the Government of Canada through Genome Canada and the Ontario Genomics Institute (OGI-148). This study was funded by the Government of Ontario.

Author contributions

O.L., T.J.M., C.E.B and T.G designed the experiments; O.L and C.B performed the experiments and analyzed the data. H.O and T.N.A.G cultured patient samples; O.L., C.E.B and T.G wrote the paper; T.J.M and P.W.E edited the paper.

FIGURE LEGEND

FIGURE 1: F508del-CFTR is rescued by the triple combination VX-445+ VX-661+ VX-770 in nasal epithelial cells from 3 patients homozygous for F508del mutation. (A) Representative tracings show Ussing chamber measurements of CFTR function in nasal epithelial cell cultures from a CF patient bearing F508del/F508del in the absence or presence of the small molecule corrector. The upper line reflects the transepithelial potential difference measurements and the downward deflection the transepithelial resistance. (**B**) Bar graphs show the mean (±SD) of the maximal response Ieq ($\mu A/cm^2$) after stimulation with forskolin (10 µM) +/- VX-770 (l µM) of 1-2 technical replicate experiments of nasal cultures generated from 3 patients. Different pre-treatments were performed (48 hrs at 37°C): DMSO (0.1%), VX-809 (3 µM)+ VX-770 (1 µM), R-VX-445 (3 µM)+ VX-661 (3 µM)+ VX-770 (1 µM), [S]-VX-445 (3 µM)+ VX-661 (3 µM)+ VX-770 (1 µM), VX-809 (3 µM) or [R]--VX-445 (3 µM)+ VX-661 (3 µM). The symbols show single Ussing chamber experiments. Comparative analysis showed statistically significant differences between nasal epithelial cells treated with VX-809+ VX-770 and VX-445+ VX-661 as well as those treated with acute and chronic VX-770. (**C**) Bar graph shows the mean (±SD) of $IeqCFTR_{inh-172}$ ($\mu A/cm^2$) by $CFTR_{Inh-172}$ (10 µM) from the same experiments done in B. (**D**) Immunoblots of steady-state expression of Wt or F508del following treatments with CFTR modulators. Band C: mature, complex-glycosylated CFTR; Band B: immature, core-glycosylated CFTR; CNX: Calnexin. Dash-lined boxes provide an example how the area for quantification of the protein abundance was chosen. (**E**) Bars represent the mean (±SD) ratio band C/ (band C+ band B) of measured nasal epithelial cells from 3 patients. Comparative analysis showed statistically significant differences between nasal epithelial cells treated with DMSO and VX-445+ VX-661 +/- VX-770. One-way ANOVA followed by Turkey's post-hoc test was used for statistical analysis. (*$p<0.05$; **$p<0.01$, ****$p<0.0001$). Paired t-test showed statistically difference between nasal epithelial cells treated with DMSO and VX-809+ VX-770. ($^{\#}p<0.05$; $^{\#\#}p<0.01$)

FIGURE 2: Nasal epithelial cultures derived from patients homozygous for other class II CFTR mutations exhibit low CFTR function and variable levels of rescue by VX-445+ VX-

661+ VX-770. Representative tracings show Ussing chamber measurements of CFTR function in nasal epithelial cell cultures from CF patients bearing (**A**) M1101K/M1101K, (**C**) G85E/G85E and (**E**) N1303K/N1303K in the absence or presence of the small molecule corrector. Immunoblots of steady-state expression of Wt and (**B**) M1101K, (**D**) G85E, (**F**) N1303K following treatments with CFTR modulators. Band C: mature, complex-glycosylated CFTR; Band B: immature, core-glycosylated CFTR; CNX: Calnexin. (**G**) Bar graphs showing the mean (±SD) of maximal response Ieq ($\mu A/cm^2$) after stimulation by forskolin (10 µM) +/- VX-770 (l µM) for nasal epithelial cell cultures from 1-3 technical replicates of 3 patients bearing M1101K, G85E, and 2 donors bearing N1303K after pre-treatment (48 hrs at 37°C) with DMSO (0.1%), VX-809 (3 µM)+ VX-770 (1 µM), [R]-VX-445 (3 µM)+ VX-661 (3 µM)+ VX-770 (1 µM) or [S]-VX-445 (3 µM)+ VX-661 (3 µM)+ VX-770 (1 µM) (**H**) Bar graphs showing the mean $IeqCFTR_{inh\text{-}172}$ ($\mu A/cm^2$) (±SD) by $CFTR_{Inh\text{-}172}$ (10 µM) for nasal epithelial cell cultures from 1-3 technical replicates of 3 patients bearing M1101K, G85E, and 2 donors bearing N1303K. (**I**) Bar graphs showing the comparison of $IeqCFTR_{inh\text{-}172}$ ($\mu A/cm^2$) by $CFTR_{Inh\text{-}172}$ across the class II mutations: M1101K-, G85E- and N1303K-CFTR for nasal epithelial cell cultures from 1-3 technical replicates of 3 patients bearing M1101K, G85E, and 2 donors bearing N1303K. Dashed line represents the mean results of the F508del/F508del nasal cells treated with VX-445+VX-661+VX-770. (**J**) Bars represent the mean (±SD) of the ratio band C/(band C+ band B) (n=1 technical replicate of 3 patients bearing M1101K, G85E and 2 patients bearing N1303K). *p<0.05; **p<0.01; ***p<0.001; ****p<0.000. Analysis was done by one-way ANOVA followed by Turkey's post-hoc test. Dashed line represents the mean results of the F508del/F508del nasal epithelial cells treated with [S]-VX-445 + VX-661 + VX-770. Paired t-test showed statistically difference between nasal epithelial cells treated with DMSO and VX-809+ VX-770. ($^{\#}p<0.05$; $^{\#\#}p<0.01$)

FIGURE 3: VX-445 compound increased channel activation of Wt-CFTR in nasal and bronchial epithelial cells. (A) Representative tracings show Ussing chamber measurements of CFTR function in nasal epithelial cell cultures from a non-CF donor. (**B**) Bar graphs showing the fold increased forskolin (10 µM) + [S]-VX-445 (3 µM) activated ΔIeq compared to forskolin (10 µM) control in 1-2 technical replicated nasal epithelial cells generated from 4 healthy controls. **(C)** Bar graphs showing the fold increased forskolin (10 µM) +/- [S]-VX-445 (3 µM) activated ΔIeq compared to forskolin (10 µM) control in bronchial epithelial cells from 4 donors (n=4). Bar graphs showing the fold increase in $IeqCFTR_{inh\text{-}172}$ ($\mu A/cm^2$) (mean ±SD) by $CFTR_{Inh\text{-}172}$ (10 µM) in (**D**) nasal epithelial cultures and (**E**) bronchial epithelial cell cultures. (**F**) Representative tracings show

Ussing chamber measurements of CFTR function in nasal epithelial cell cultures from a CF patient homozygous for F508del mutation following treatment with 48 hrs of VX-661 (3 μM). $CFTR_{Inh-172}$ (10 μM) was given repeatedly to ensure complete inhibition of CFTR. (**G**) Bar graphs showing the fold increased forskolin (10 μM) + [S]-VX-445 (3 μM) activated ΔIeq compared to forskolin (10 μM) control in 2 technical replicate of nasal epithelial cells generated from 2 CF donors homozygous for F508del. (**H**) Bar graphs showing the corresponding fold increased in $IeqCFTR_{inh-172}$ ($\mu A/cm^2$) (mean ±SD) by $CFTR_{Inh-172}$ (10 μM). Comparative analysis was performed using paired two-tailed Student's t-test. Statistically significant difference is shown between untreated cells and those with acute treatment of [S]-VX-445. *p<0.05; ***p<0.001.

FIGURE 4: VX-445 potentiates temperature rescued F508del-, M1101K and N1303K-CFTR in HEK293 cells. (**A**) Representative traces of F508del-CFTR dependent chloride efflux (membrane depolarization assay, 3 μM [S]-VX-445 + 10 μM forskolin) in HEK293 cells stable transfected with F508del-CFTR after 24 h incubation at 27°C. Dose-response of VX-770 or [S]-VX-445 (0.001-3 μM) + forskolin (10 μM) (±SD) in (**B**) F508del, (**C**) M1101K or (**D**) N1303K-CFTR HEK293 cells (n= 5 biological replicates and 4 technical replicates for each experiment)**.** *p<0.05; **p<0.01, ***p<0.001 by one way ANOVA followed by Turkey's post-hoc test.

FIGURE 5: F508del-CFTR and other rare CFTR mutations expressed in HEK293 cells rescued by VX-445+ VX-661+ VX-770. (**A**) Representative traces of F508del-CFTR dependent chloride efflux (membrane depolarization assay) in HEK293 cells stable transfected with F508del-CFTR pre-treated with DMSO or [S]-VX-445 (3 μM) + VX-661 (3 μM) for 24 hrs at 37°C. (**B**) Bar graphs show the mean (±SD) of maximal activation of F508del-CFTR after stimulation by FSK (1 0μM) +/- VX-770 (1 μM) and/or [S]-VX-445 (1 μM). (**C**) HEK293 were transiently transfected with M1101K-, G85E or N1303K and treated for 24 hrs at 37°C with: DMSO, VX-809 (3 μM), VX-661 (3 μM) or [S]-VX-445 (3 μM) + VX-661 (3 μM). Bar graphs show the mean (±SD) of maximal activation of M1101K, G85E and N1303K-CFTR after stimulation by FSK (10 μM) +/- VX-770 (1 μM) and/or [S]-VX-445 (1 μM) (n=3-10). (**D**) Immunoblots of steady-state expression of F508del, M1101K, G85E or N1303K-CFTR following treatments for 24 hrs at 37°C with: DMSO, VX-809 (3 μM), VX-661 (3 μM) or [S]-VX-445 (3 μM) + VX-661 (3 μM). C: mature, complex-glycosylated CFTR; B: immature, core-glycosylated CFTR; CNX, Calnexin. (**E**) Bars represent the mean (±SD) of the ratio band C/(band C+ band B) (n=3). Comparative analysis was performed using by one-way ANOVA followed by Turkey's post-hoc test. *p<0.05, **p<0.01; ***p<0.001; ****p<0.0001

FIGURE S1: ORKAMBI™ and SYMDEKO™ showed similar rescue of F508del-CFTR in nasal epithelial cultures derived from 6 patients homozygous for F508del/F508del. (**A**) Representative tracing show Ussing chamber studies measurements of CFTR function in nasal epithelial cell cultures from F508del/F508del patients after pre-treatment with DMSO, VX-809 (3 µM) or VX-661 (3 µM). (**B**) Bar graphs showing the mean (±SD) of maximal response Ieq ($\mu A/cm^2$) after stimulation with forskolin (10 µM) + VX-770 (l µM) (2 inserts for each treatment). (**C**) Bar graphs showing the $IeqCFTR_{inh-172}$ ($\mu A/cm^2$) by $CFTR_{Inh-172}$ (10 µM). Comparative analysis was performed using by one-way ANOVA followed by Turkey's post-hoc test. *$p<0.05$.

FIGURE S2: VX-445 compound increased channel activation of Wt-CFTR in nasal epithelial cells. (A) Representative trace showing Ussing chamber measurements of CFTR function in nasal epithelial cell cultures from a non-CF donor. (**B**) Bar graphs showing the fold increased forskolin (0.1 µM) + [S]-VX-445 (3 µM) activated ΔIeq compared to forskolin (0.1 µM) control in 3 technical replicated nasal epithelial cells generated from 1 healthy control. *$p<0.05$.

FIGURE S3: VX-445+ VX-661+ VX-770 showed functional rescue of N1303K-CFTR in CFF 16HBEge CFTR-N1303K. (A) Representative traces of N1303K-CFTR-dependent chloride efflux by FLIPR assay in HBE cells pre-treated with DMSO, VX-809 (3 µM), [S]-VX-445 (3 µM)+ VX-661 (3 µM), VX-661 (3 µM)+ VX-770 (1 µM) or [S]-VX-445 (3 µM)+ VX-661 (3 µM)+ VX-770 (1 µM) for 24 hrs at 37°C. (**B**) Bar graphs show the mean (±SD) of maximal activation of N1303K-CFTR after stimulation by FSK (10 µM) +/- VX-770 (1 µM) (n= 4 biological replicates and 4 technical replicates for each experiment) *$p<0.05$; ****$p<0.0001$ by one way ANOVA followed by Turkey's post-hoc test.

FIGURE S4: VX-445+ VX-661+ VX-770 failed to rescue Y569D-CFTR channel activity in nasal epithelial cultures derived from 1 patient homozygous for Y569D/Y569D. (A) Representative tracings show Ussing chamber measurements of CFTR function in nasal epithelial cell cultures from 1 CF patient bearing Y596D/Y569D in the absence or presence of the [S]-VX-445+ VX-661+ VX-770. (**B**) Bar graphs showing the mean (±SD) of maximal response Ieq ($\mu A/cm^2$) after stimulation by forskolin (10 µM) +/- VX-770 (l µM) for nasal cultures from 1 patient bearing Y596D/Y569D after pre-treatment (48 hrs at 37°C) with DMSO (0.1%) or [S]-VX-445 (3 µM)+ VX-661 (3 µM)+ VX-770 (1 µM) (2 inserts for each treatment). (**C**) Bar graphs showing the IeqCFTR inhibition ($\mu A/cm^2$) by $CFTR_{Inh-172}$ (10 µM) (2 inserts for each treatment).

(**D**) Immunoblots of steady-state expression of Wt or Y596D/Y569D following treatments with CFTR modulators. Band C: mature, complex-glycosylated CFTR; Band B: immature, core-glycosylated CFTR; CNX: Calnexin. (**E**) Bars represent the ratio of band C/(band C+ band B) (n=2). Statistical analysis was performed using paired two-tailed Student's t-test.

FIGURE S5: VX-445+ VX-661+ VX-770 showed minimal increase in CFTR activity in nasal epithelial cultures derived from patients with G542X/N1303K mutation (n=2). (A) Representative tracings show Ussing chamber measurements of CFTR function in nasal epithelial cell cultures from a CF patient bearing G542X/N1303K in the absence or presence of the small molecule corrector. (**B**) Bar graphs showing the mean (±SD) of maximal response Ieq ($\mu A/cm^2$) after stimulation by forskolin (10 µM) +/- VX-770 (l µM) of 1-2 technical replicates of nasal epithelial cell cultures generated from 2 patients bearing G542X/N1303K. Nasal epithelial cells were treated (48h at 37°C) with DMSO (0.1%), VX-809 (3 µM)+ VX-770 (1 µM), R-VX-445 (3 µM)+ VX-661 (3 µM)+ VX-770 (1 µM) or [S]-VX-445 (3 µM)+ VX-661 (3 µM)+ VX-770 (1 µM) (2-3 inserts for each treatment). (**C**) Bar graphs showing the mean (±SD) $IeqCFTR_{inh-172}$ ($\mu A/cm^2$) by $CFTR_{Inh-172}$ (10 µM). (**D**) Immunoblots of steady-state expression of G542X/N1303K following treatments with CFTR modulators. Band C: mature, complex-glycosylated CFTR; Band B: immature, core-glycosylated CFTR; CNX: Calnexin. (**E**) Bars represent the mean (±SD) of the ratio band C/(band C+ band B) (n=2). Statistical analysis was performed using one-way ANOVA followed by Turkey's post-hoc test.

REFERENCES

1. Riordan, J.R., et al., *Identification of the cystic fibrosis gene: cloning and characterization of complementary DNA.* Science, 1989. **245**(4922): p. 1066-73.
2. Bear, C.E., et al., *Purification and functional reconstitution of the cystic fibrosis transmembrane conductance regulator (CFTR).* Cell, 1992. **68**(4): p. 809-18.
3. Rowe, S.M., S. Miller, and E.J. Sorscher, *Cystic fibrosis.* N Engl J Med, 2005. **352**(19): p. 1992-2001.
4. Wainwright, C.E., et al., *Lumacaftor-Ivacaftor in Patients with Cystic Fibrosis Homozygous for Phe508del CFTR.* N Engl J Med, 2015. **373**(3): p. 220-31.
5. Ramsey, B.W., et al., *A CFTR potentiator in patients with cystic fibrosis and the G551D mutation.* N Engl J Med, 2011. **365**(18): p. 1663-72.

6. Taylor-Cousar, J.L., et al., *Tezacaftor-Ivacaftor in Patients with Cystic Fibrosis Homozygous for Phe508del.* N Engl J Med, 2017. **377**(21): p. 2013-2023.
7. Keating, D., et al., *VX-445-Tezacaftor-Ivacaftor in Patients with Cystic Fibrosis and One or Two Phe508del Alleles.* N Engl J Med, 2018. **379**(17): p. 1612-1620.
8. Guerra, L., et al., *The preclinical discovery and development of the combination of ivacaftor + tezacaftor used to treat cystic fibrosis.* Expert Opin Drug Discov, 2020. **15**(8): p. 873-891.
9. Middleton, P.G., et al., *Elexacaftor-Tezacaftor-Ivacaftor for Cystic Fibrosis with a Single Phe508del Allele.* N Engl J Med, 2019. **381**(19): p. 1809-1819.
10. Molinski, S., et al., *Functional Rescue of F508del-CFTR Using Small Molecule Correctors.* Front Pharmacol, 2012. **3**: p. 160.
11. Rapino, D., et al., *Rescue of NBD2 mutants N1303K and S1235R of CFTR by small-molecule correctors and transcomplementation.* PLoS One, 2015. **10**(3): p. e0119796.
12. Lopes-Pacheco, M., et al., *Combination of Correctors Rescues CFTR Transmembrane-Domain Mutants by Mitigating their Interactions with Proteostasis.* Cell Physiol Biochem, 2017. **41**(6): p. 2194-2210.
13. Liu, Q., et al., *Rescue of CFTR NBD2 mutants N1303K and S1235R is influenced by the functioning of the autophagosome.* J Cyst Fibros, 2018. **17**(5): p. 582-594.
14. DeStefano, S., M. Gees, and T.C. Hwang, *Physiological and pharmacological characterization of the N1303K mutant CFTR.* J Cyst Fibros, 2018. **17**(5): p. 573-581.
15. Han, S.T., et al., *Residual function of cystic fibrosis mutants predicts response to small molecule CFTR modulators.* JCI Insight, 2018. **3**(14).
16. Eckford, P.D.W., et al., *The CF Canada-Sick Kids Program in individual CF therapy: A resource for the advancement of personalized medicine in CF.* J Cyst Fibros, 2019. **18**(1): p. 35-43.
17. Laselva, O., et al., *The CFTR Mutation c.3453G > C (D1152H) Confers an Anion Selectivity Defect in Primary Airway Tissue that Can Be Rescued by Ivacaftor.* J Pers Med, 2020. **10**(2).
18. Laselva, O., et al., *Activity of lumacaftor is not conserved in zebrafish Cftr bearing the major cystic fibrosis-causing mutation.* FASEB Bioadv, 2019. **1**(10): p. 661-670.
19. Valley, H.C., et al., *Isogenic cell models of cystic fibrosis-causing variants in natively expressing pulmonary epithelial cells.* J Cyst Fibros, 2019. **18**(4): p. 476-483.
20. Wu, Y.S., et al., *ORKAMBI-Mediated Rescue of Mucociliary Clearance in Cystic Fibrosis Primary Respiratory Cultures Is Enhanced by Arginine Uptake, Arginase Inhibition, and Promotion of Nitric Oxide Signaling to the Cystic Fibrosis Transmembrane Conductance Regulator Channel.* Mol Pharmacol, 2019. **96**(4): p. 515-525.
21. Cao, H., et al., *A helper-dependent adenoviral vector rescues CFTR to wild type functional levels in CF epithelial cells harbouring class I mutations.* Eur Respir J, 2020.
22. Molinski, S.V., et al., *Orkambi(R) and amplifier co-therapy improves function from a rare CFTR mutation in gene-edited cells and patient tissue.* EMBO Mol Med, 2017. **9**(9): p. 1224-1243.
23. Laselva, O., et al., *Preclinical Studies of a Rare CF-Causing Mutation in the Second Nucleotide Binding Domain (c.3700A>G) Show Robust Functional Rescue in Primary Nasal Cultures by Novel CFTR Modulators.* J Pers Med, 2020. **10**(4).
24. Erwood, S., et al., *Allele-Specific Prevention of Nonsense-Mediated Decay in Cystic Fibrosis Using Homology-Independent Genome Editing.* Mol Ther Methods Clin Dev, 2020. **17**: p. 1118-1128.
25. Laselva, O., et al., *Anti-Infectives Restore ORKAMBI((R)) Rescue of F508del-CFTR Function in Human Bronchial Epithelial Cells Infected with Clinical Strains of P. aeruginosa.* Biomolecules, 2020. **10**(2).

26. Cao, H., et al., *Testing gene therapy vectors in human primary nasal epithelial cultures.* Mol Ther Methods Clin Dev, 2015. **2**: p. 15034.
27. Laselva, O., et al., *Functional rescue of c.3846G>A (W1282X) in patient-derived nasal cultures achieved by inhibition of nonsense mediated decay and protein modulators with complementary mechanisms of action.* J Cyst Fibros, 2019.
28. Chin, S., et al., *Cholesterol Interaction Directly Enhances Intrinsic Activity of the Cystic Fibrosis Transmembrane Conductance Regulator (CFTR).* Cells, 2019. **8**(8).
29. Laselva, O., et al., *Molecular Mechanism of Action of Trimethylangelicin Derivatives as CFTR Modulators.* Front Pharmacol, 2018. **9**: p. 719.
30. Molinski, S.V., et al., *Comprehensive mapping of cystic fibrosis mutations to CFTR protein identifies mutation clusters and molecular docking predicts corrector binding site.* Proteins, 2018. **86**(8): p. 833-843.
31. Laselva, O., et al., *Correctors of the Major Cystic Fibrosis Mutant Interact through Membrane-Spanning Domains.* Mol Pharmacol, 2018. **93**(6): p. 612-618.
32. Cholon, D.M., et al., *Potentiator ivacaftor abrogates pharmacological correction of DeltaF508 CFTR in cystic fibrosis.* Sci Transl Med, 2014. **6**(246): p. 246ra96.
33. Veit, G., et al., *Some gating potentiators, including VX-770, diminish DeltaF508-CFTR functional expression.* Sci Transl Med, 2014. **6**(246): p. 246ra97.
34. Cui, G., et al., *VX-770-mediated potentiation of numerous human CFTR disease mutants is influenced by phosphorylation level.* Sci Rep, 2019. **9**(1): p. 13460.
35. Laselva, O., et al., *Emerging preclinical modulators developed for F508del-CFTR have the potential to be effective for ORKAMBI resistant processing mutants.* J Cyst Fibros, 2020.
36. Heijerman, H.G.M., et al., *Efficacy and safety of the elexacaftor plus tezacaftor plus ivacaftor combination regimen in people with cystic fibrosis homozygous for the F508del mutation: a double-blind, randomised, phase 3 trial.* Lancet, 2019. **394**(10212): p. 1940-1948.
37. Veit, G., et al., *Allosteric folding correction of F508del and rare CFTR mutants by elexacaftor-tezacaftor-ivacaftor (Trikafta) combination.* JCI Insight, 2020. **5**(18).
38. Phuan, P.W., et al., *Nanomolar-potency 'co-potentiator' therapy for cystic fibrosis caused by a defined subset of minimal function CFTR mutants.* Sci Rep, 2019. **9**(1): p. 17640.
39. Phuan, P.W., et al., *Combination potentiator ('co-potentiator') therapy for CF caused by CFTR mutants, including N1303K, that are poorly responsive to single potentiators.* J Cyst Fibros, 2018. **17**(5): p. 595-606.

FIGURE 1

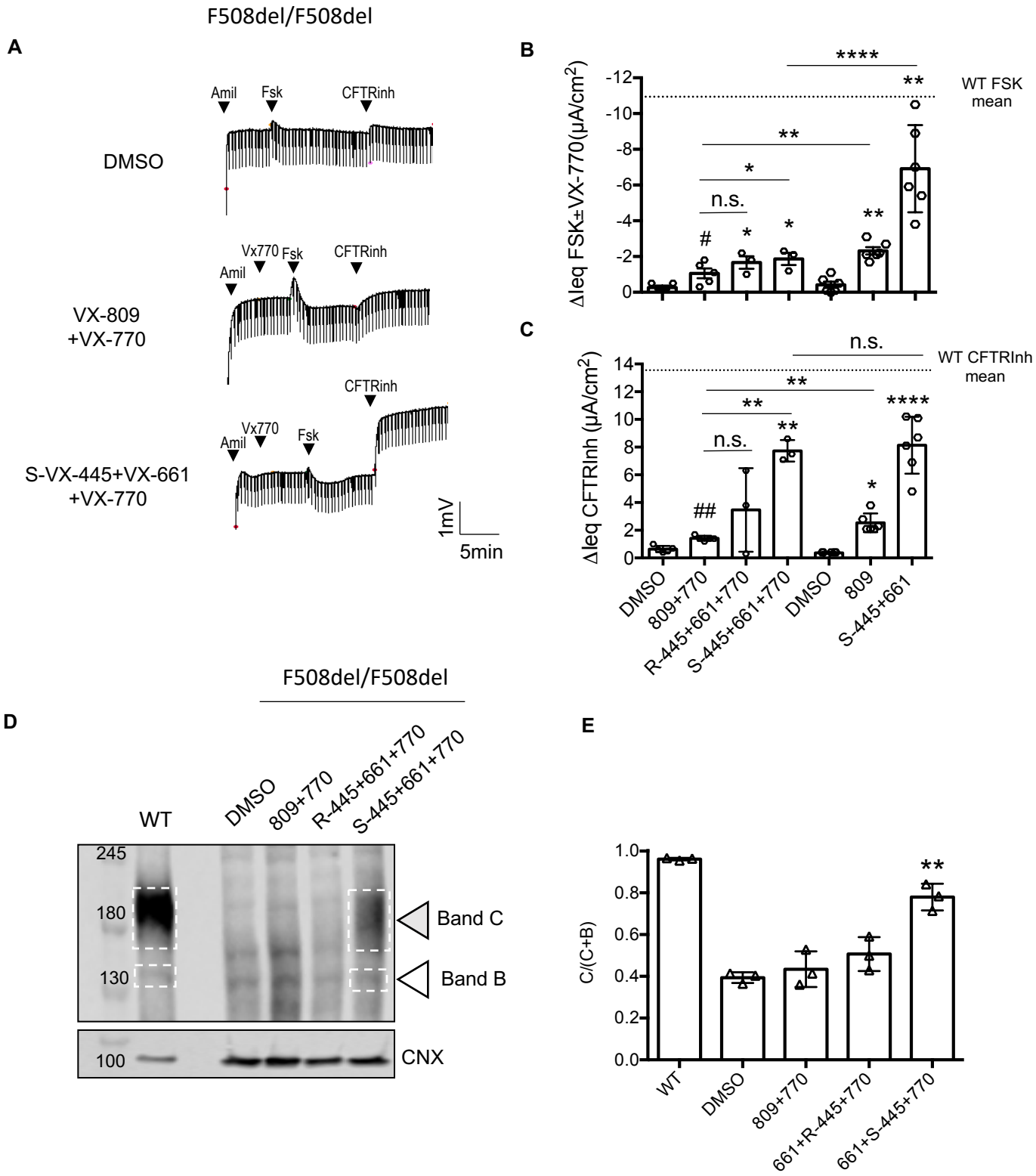
F508del/F508del
A
Amil
Fsk
CFTRinh
DMSO
Vx770
Fsk
CFTRinh
Amil
VX-809
+VX-770
CFTRinh
Vx770
Amil
Fsk
S-VX-445+VX-661
+VX-770
1mV
5min
B
ΔIeq FSK±VX-770(μA/cm²)
WT FSK
mean
n.s.
C
ΔIeq CFTRInh (μA/cm²)
WT CFTRInh
mean
n.s.
DMSO
809+770
R-445+661+770
S-445+661+770
DMSO
809
S-445+661
F508del/F508del
D
WT
DMSO
809+770
R-445+661+770
S-445+661+770
245
180
130
Band C
Band B
100
CNX
E
C/(C+B)
WT
DMSO
809+770
661+R-445+770
661+S-445+770

FIGURE 2

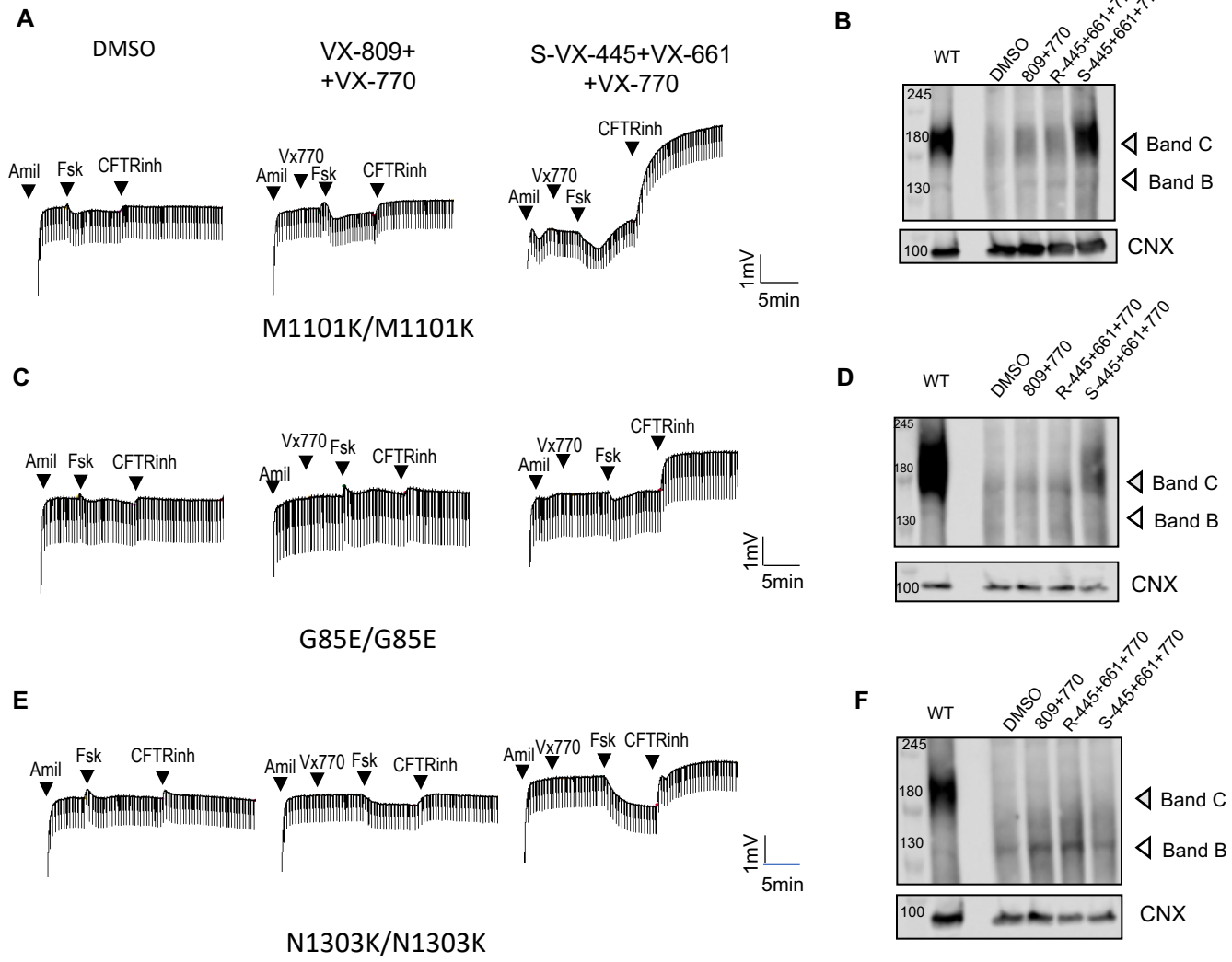
A
DMSO
VX-809+
+VX-770
S-VX-445+VX-661
+VX-770
Amil
Fsk
CFTRinh
Vx770
1mV
5min
M1101K/M1101K
B
WT
DMSO
809+770
R-445+661+770
S-445+661+770
245
180
130
100
Band C
Band B
CNX
C
G85E/G85E
D
E
N1303K/N1303K
F

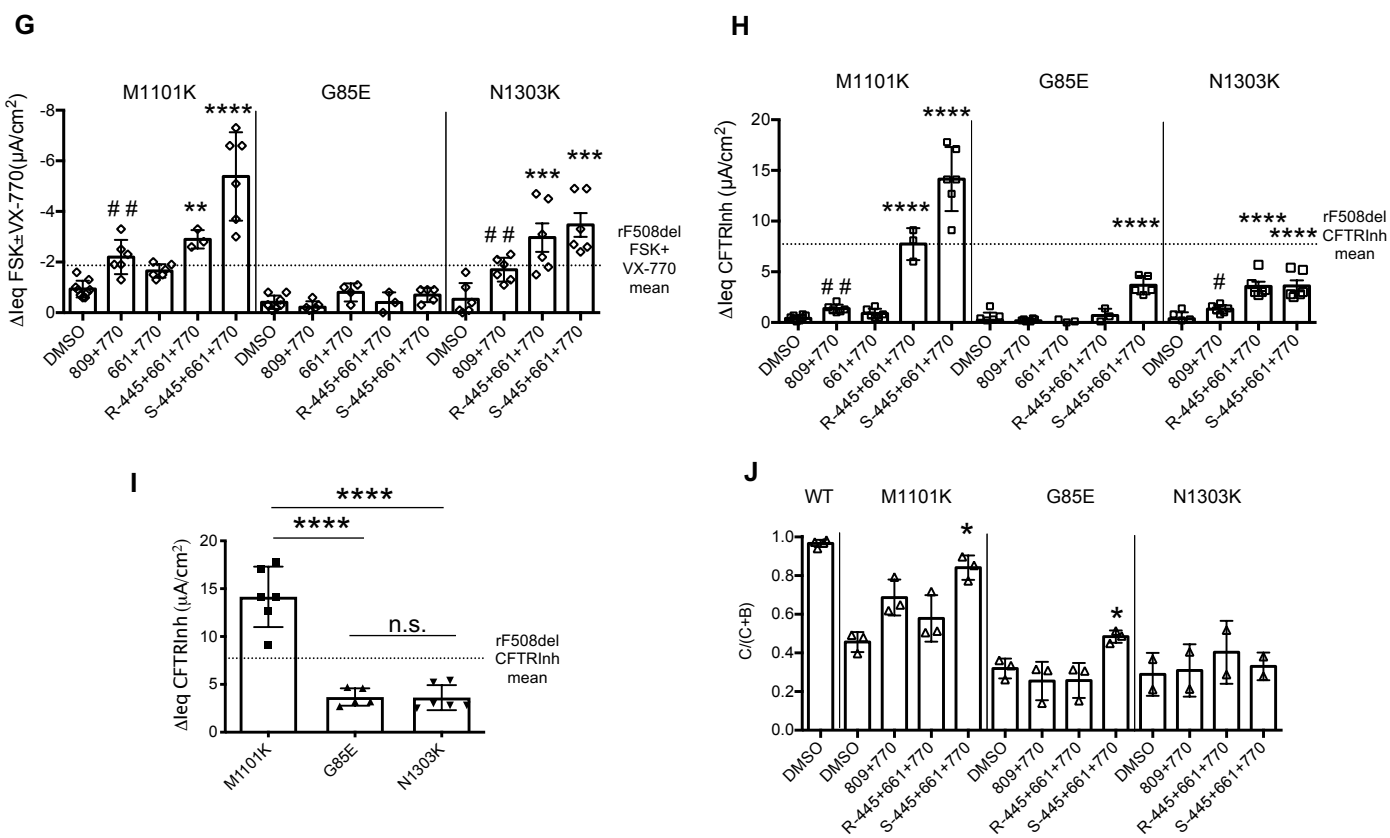
G
M1101K
G85E
N1303K
ΔIeq FSK±VX-770(μA/cm²)
rF508del
FSK+
VX-770
mean
DMSO
809+770
661+770
R-445+661+770
S-445+661+770
H
ΔIeq CFTRInh (μA/cm²)
rF508del
CFTRInh
mean
I
n.s.
J
WT
C/(C+B)

FIGURE 3

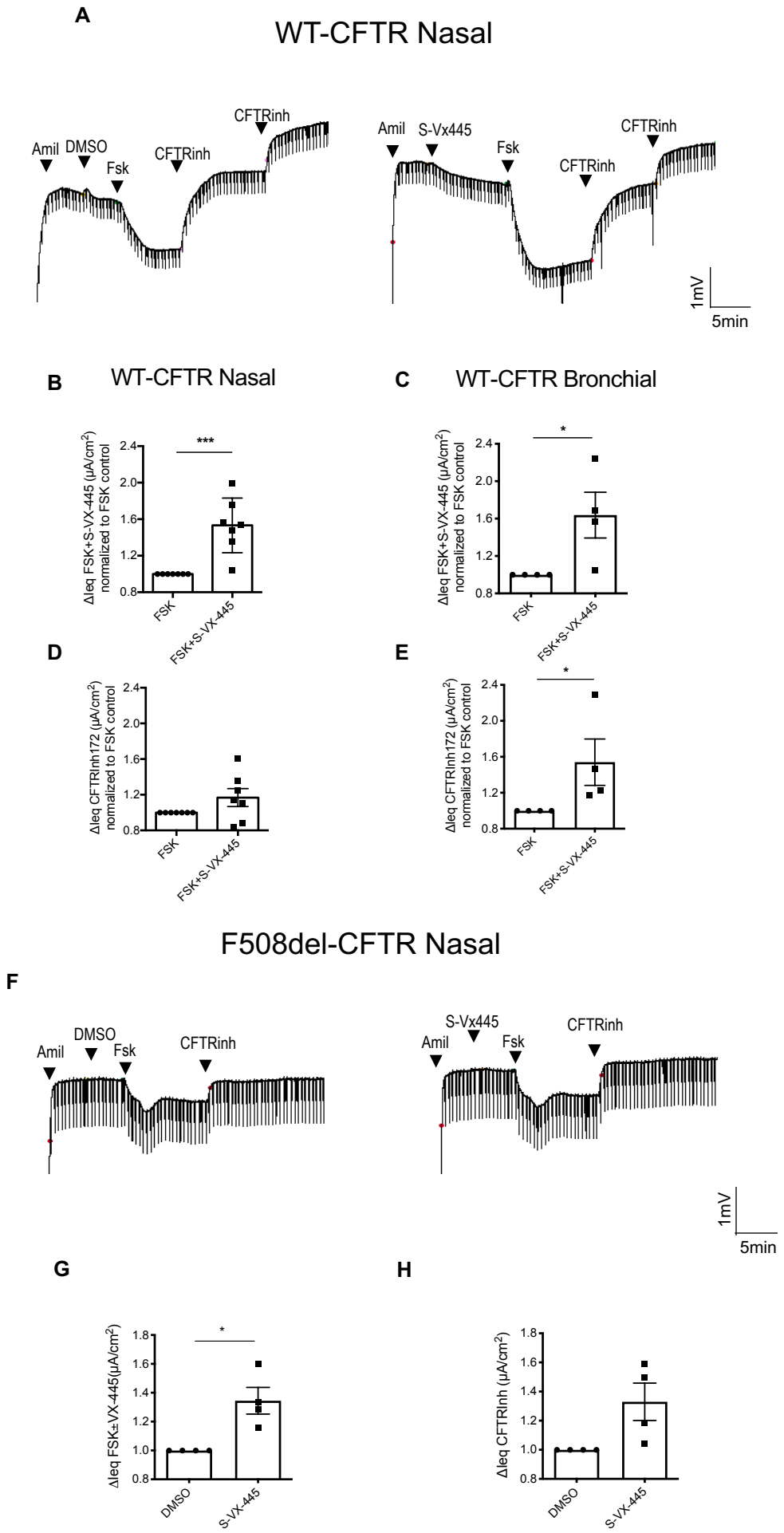
A
WT-CFTR Nasal
Amil
DMSO
Fsk
CFTRinh
CFTRinh
Amil
S-Vx445
Fsk
CFTRinh
1mV
5min
B
WT-CFTR Nasal
C
WT-CFTR Bronchial
Δleq FSK+S-VX-445 (μA/cm²) normalized to FSK control
***
*
FSK
FSK+S-VX-445
D
E
Δleq CFTRInh172 (μA/cm²) normalized to FSK control
F508del-CFTR Nasal
F
G
H
Δleq FSK± VX-445(μA/cm²)
Δleq CFTRInh (μA/cm²)
DMSO
S-VX-445

FIGURE 4

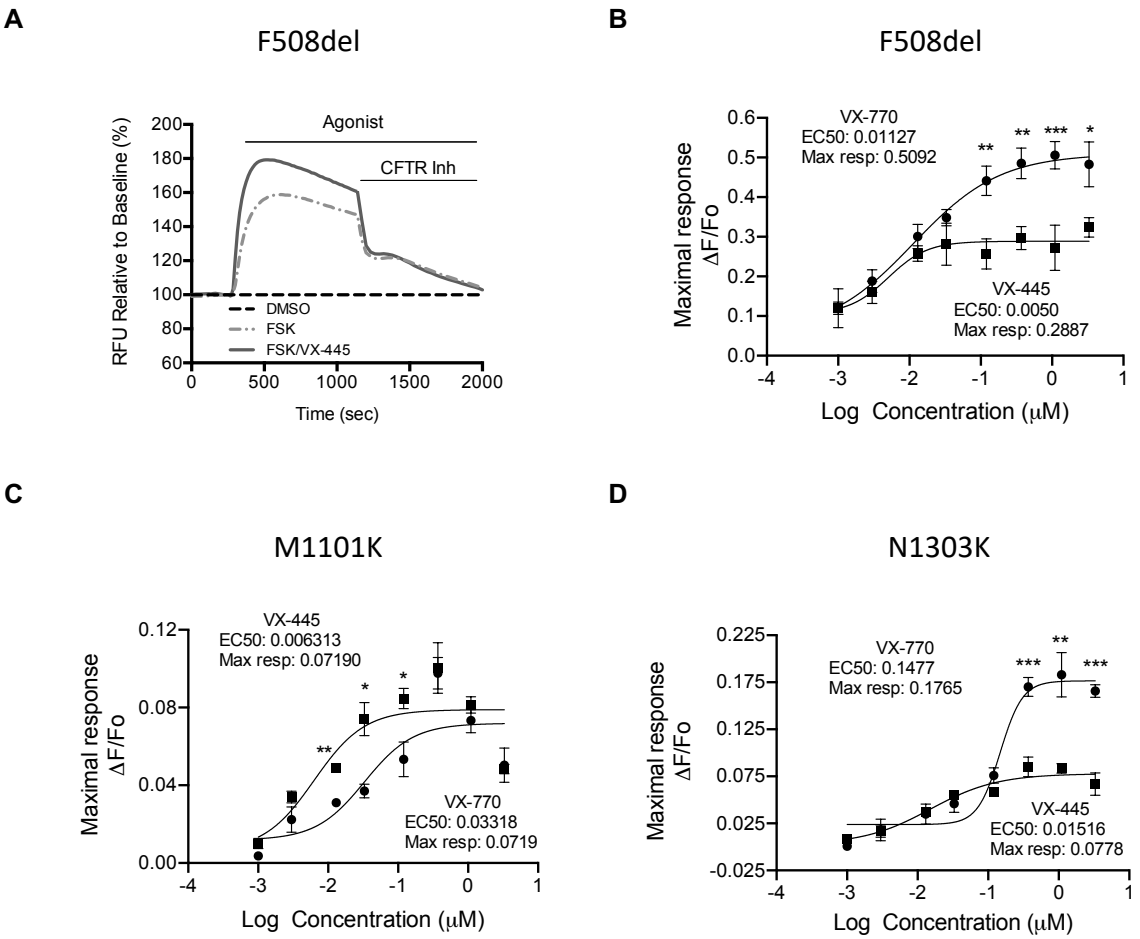
A
F508del
Agonist
CFTR Inh
RFU Relative to Baseline (%)
DMSO
FSK
FSK/VX-445
Time (sec)
B
F508del
VX-770
EC50: 0.01127
Max resp: 0.5092
VX-445
EC50: 0.0050
Max resp: 0.2887
Maximal response ΔF/Fo
Log Concentration (μM)
C
M1101K
VX-445
EC50: 0.006313
Max resp: 0.07190
VX-770
EC50: 0.03318
Max resp: 0.0719
Maximal response ΔF/Fo
Log Concentration (μM)
D
N1303K
VX-770
EC50: 0.1477
Max resp: 0.1765
VX-445
EC50: 0.01516
Max resp: 0.0778
Maximal response ΔF/Fo
Log Concentration (μM)

FIGURE 5

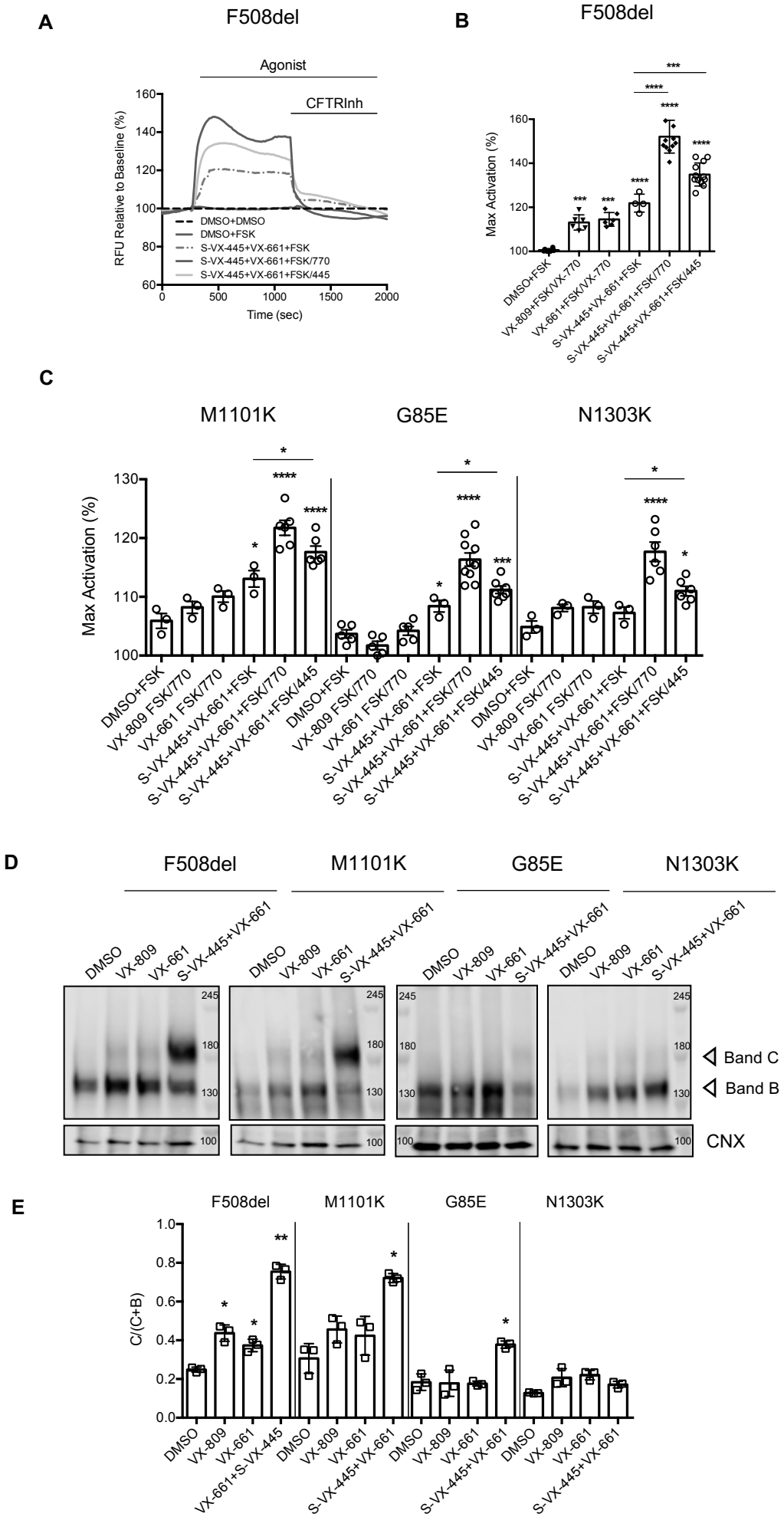
A
F508del
Agonist
CFTRInh
RFU Relative to Baseline (%)
Time (sec)
DMSO+DMSO
DMSO+FSK
S-VX-445+VX-661+FSK
S-VX-445+VX-661+FSK/770
S-VX-445+VX-661+FSK/445
B
F508del
Max Activation (%)
DMSO+FSK
VX-809+FSK/VX-770
VX-661+FSK/VX-770
S-VX-445+VX-661+FSK
S-VX-445+VX-661+FSK/770
S-VX-445+VX-661+FSK/445
C
M1101K
G85E
N1303K
Max Activation (%)
DMSO+FSK
VX-809 FSK/770
VX-661 FSK/770
S-VX-445+VX-661+FSK
S-VX-445+VX-661+FSK/770
S-VX-445+VX-661+FSK/445
D
F508del
M1101K
G85E
N1303K
DMSO
VX-809
VX-661
S-VX-445+VX-661
Band C
Band B
CNX
E
F508del
M1101K
G85E
N1303K
C/(C+B)
DMSO
VX-809
VX-661
VX-661+S-VX-445
S-VX-445+VX-661

FIGURE S1

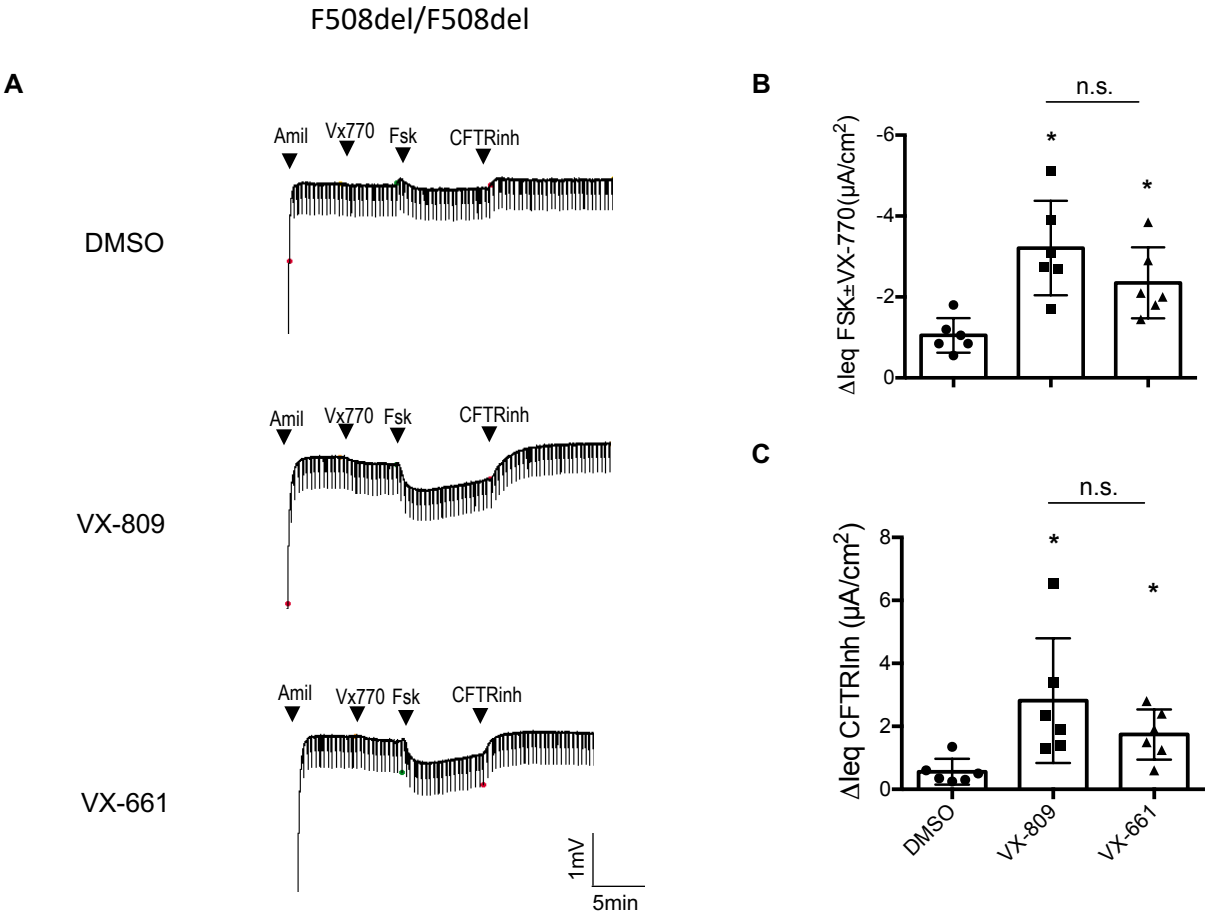
F508del/F508del
A
Amil
Vx770
Fsk
CFTRinh
DMSO
VX-809
VX-661
1mV
5min
B
n.s.
ΔIeq FSK±VX-770(μA/cm²)
-6
-4
-2
0
C
n.s.
ΔIeq CFTRInh (μA/cm²)
8
6
4
2
0
DMSO
VX-809
VX-661

FIGURE S2

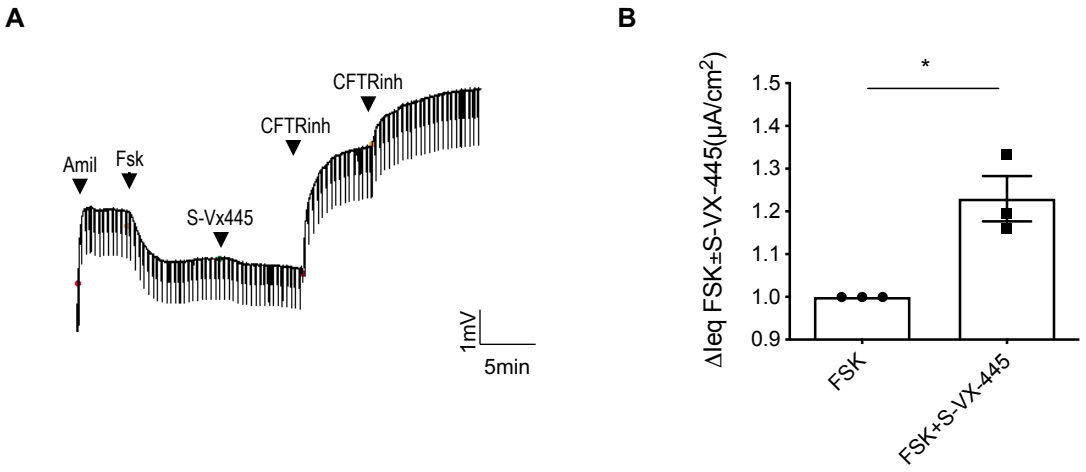
A
Amil
Fsk
S-Vx445
CFTRinh
CFTRinh
1mV
5min
B
*
ΔIeq FSK±S-VX-445(μA/cm²)
1.5
1.4
1.3
1.2
1.1
1.0
0.9
FSK
FSK+S-VX-445

FIGURE S3

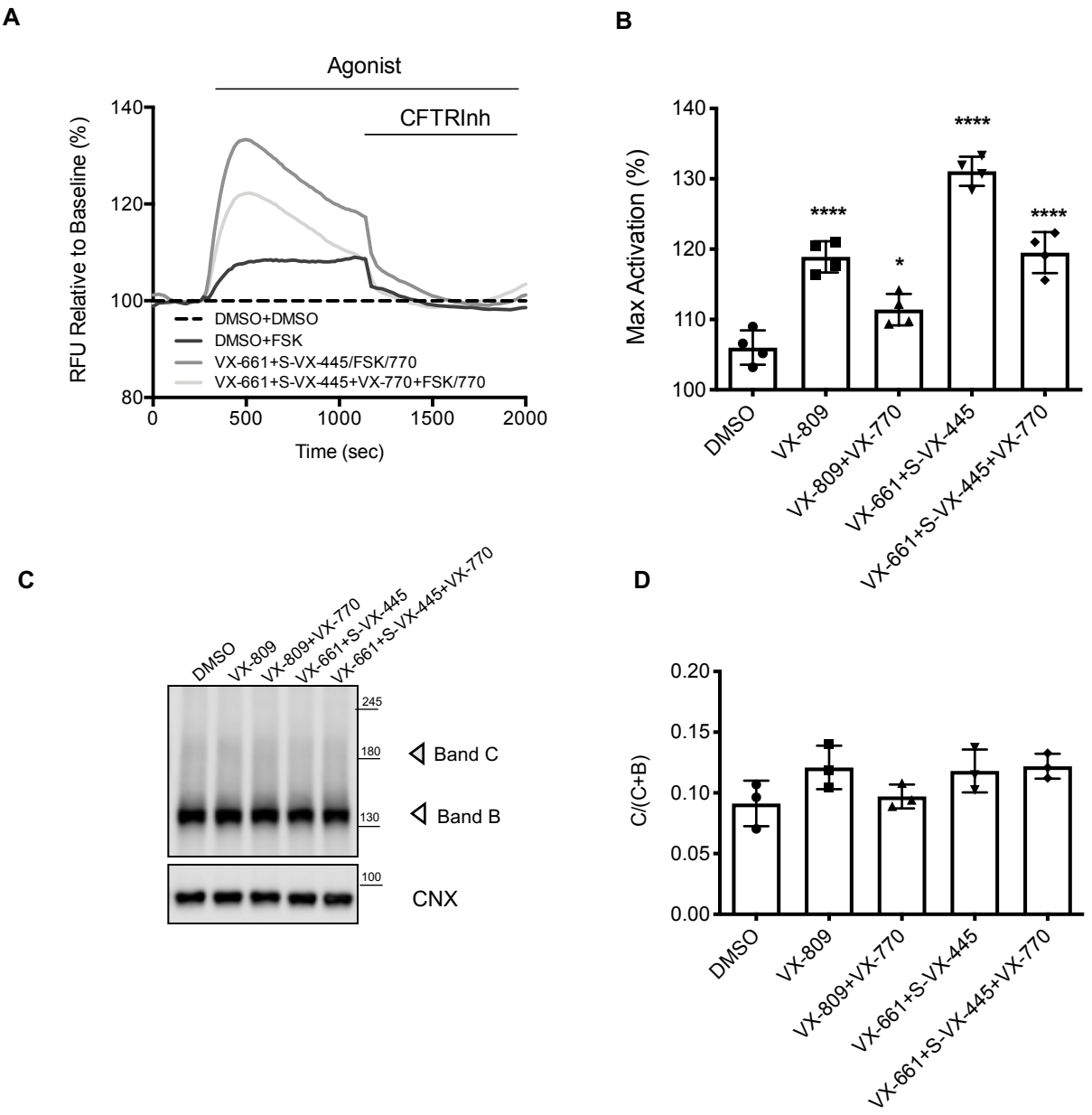
A
Agonist
CFTRInh
RFU Relative to Baseline (%)
140
120
100
80
0
500
1000
1500
2000
Time (sec)
DMSO+DMSO
DMSO+FSK
VX-661+S-VX-445/FSK/770
VX-661+S-VX-445+VX-770+FSK/770
B
Max Activation (%)
140
130
120
110
100
****
*
****
****
DMSO
VX-809
VX-809+VX-770
VX-661+S-VX-445
VX-661+S-VX-445+VX-770
C
DMSO
VX-809
VX-809+VX-770
VX-661+S-VX-445
VX-661+S-VX-445+VX-770
245
180
130
100
Band C
Band B
CNX
D
C/(C+B)
0.20
0.15
0.10
0.05
0.00
DMSO
VX-809
VX-809+VX-770
VX-661+S-VX-445
VX-661+S-VX-445+VX-770

FIGURE S4

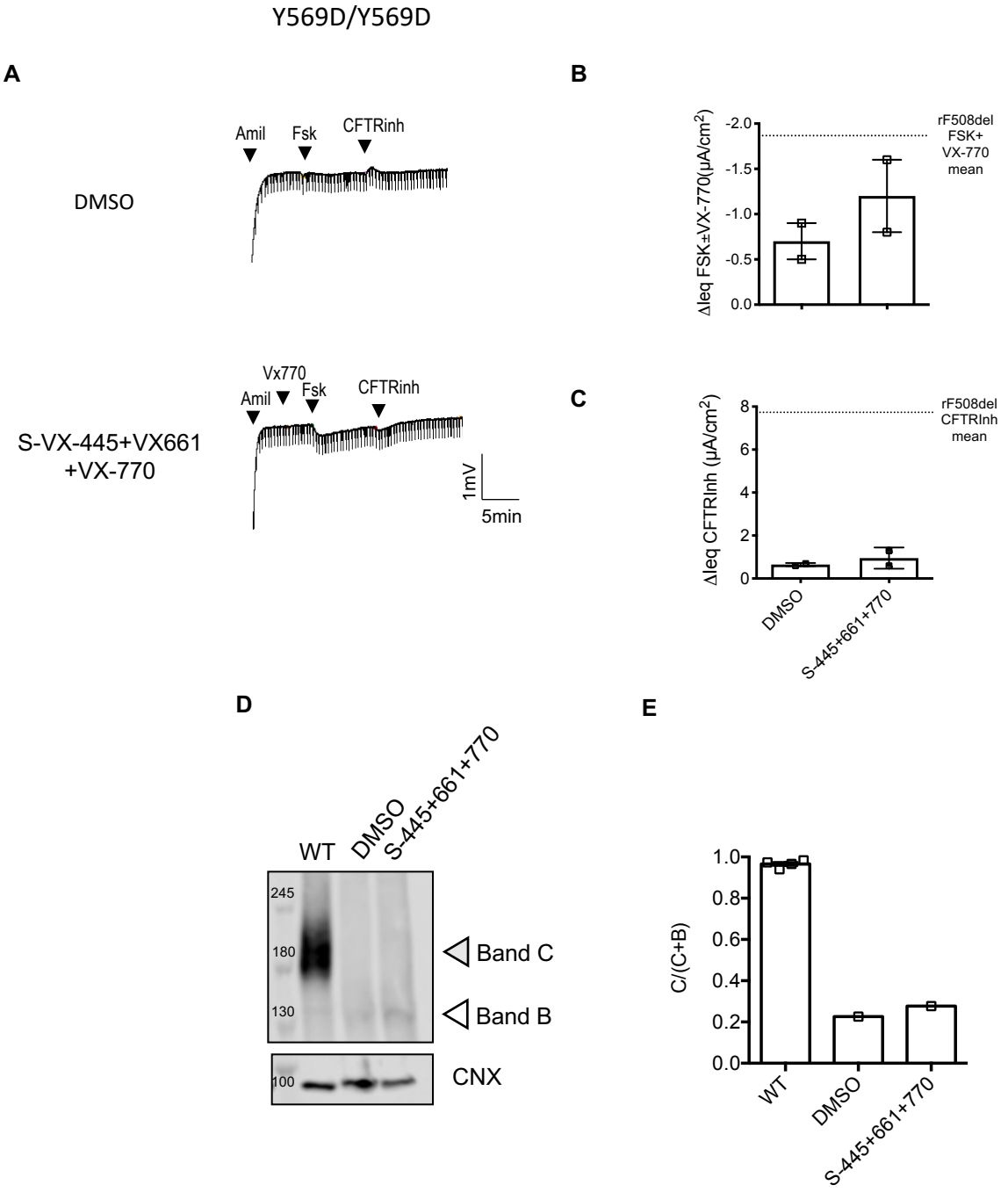
Y569D/Y569D
A
DMSO
Amil
Fsk
CFTRinh
S-VX-445+VX661
+VX-770
Vx770
1mV
5min
B
ΔIeq FSK±VX-770(μA/cm²)
rF508del
FSK+
VX-770
mean
C
ΔIeq CFTRInh (μA/cm²)
rF508del
CFTRInh
mean
DMSO
S-445+661+770
D
WT
DMSO
S-445+661+770
245
180
130
Band C
Band B
100
CNX
E
C/(C+B)
WT
DMSO
S-445+661+770

FIGURE S5

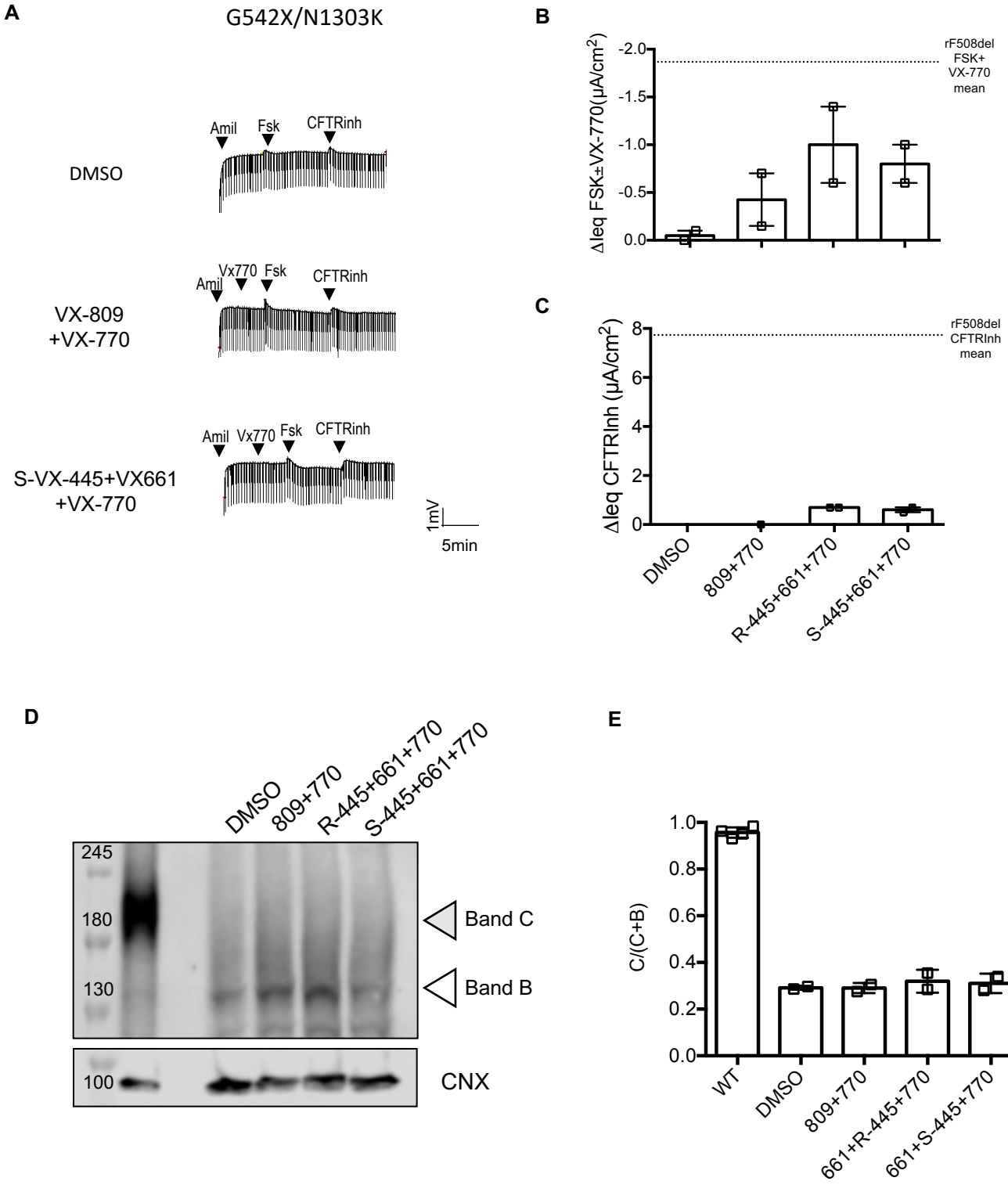
A
G542X/N1303K
DMSO
Amil
Fsk
CFTRinh
VX-809
+VX-770
Vx770
S-VX-445+VX661
+VX-770
1mV
5min
B
ΔIeq FSK±VX-770(μA/cm²)
rF508del
FSK+
VX-770
mean
C
ΔIeq CFTRInh (μA/cm²)
rF508del
CFTRInh
mean
DMSO
809+770
R-445+661+770
S-445+661+770
D
245
180
130
100
Band C
Band B
CNX
E
C/(C+B)
WT
661+R-445+770
661+S-445+770